Available online at www.sciencedirect.com
ScienceDirect
Physics Letters B 650 (2007) 135–140
PHYSICS LETTERS B
www.elsevier.com/locate/physletb

One-particle excitations outside the ^{54}Ti semi-magic core: The ^{55}V and ^{55}Ti yrast structures

S. Zhu [a], R.V.F. Janssens [a,*], B. Fornal [b], S.J. Freeman [c], M. Honma [d], R. Broda [b], M.P. Carpenter [a], A.N. Deacon [c], B.P. Kay [c], F.G. Kondev [e], W. Królas [b,f], J. Kozemczak [g], A. Larabee [g], T. Lauritsen [a], S.N. Liddick [h,i], C.J. Lister [a], P.F. Mantica [h,i], T. Otsuka [j,k], T. Pawłat [b], A. Robinson [a], D. Seweryniak [a], J.F. Smith [c,1], D. Steppenbeck [c], B.E. Tomlin [h,i], J. Wrzesiński [b], X. Wang [a,l]

[a] *Argonne National Laboratory, Argonne, IL 60439, USA*
[b] *Institute of Nuclear Physics, Polish Academy of Sciences, PL-31342 Krakow, Poland*
[c] *School of Physics and Astronomy, University of Manchester, Manchester M13 9PL, United Kingdom*
[d] *Center for Mathematical Sciences, University of Aizu, Tsuruga, Ikki-machi, Aizu-Wakamatsu, Fukushima 965-8580, Japan*
[e] *Nuclear Engineering Division, Argonne National Laboratory, Argonne, IL 60439, USA*
[f] *Joint Institute for Heavy Ion Research, Oak Ridge, TN 37381,USA*
[g] *Physics Department, Greenville College, Greenville, IL 62246, USA*
[h] *National Superconducting Cyclotron Laboratory, Michigan State University, East Lansing, MI 48824, USA*
[i] *Department of Chemistry, Michigan State University, East Lansing, MI 48824, USA*
[j] *Department of Physics, University of Tokyo, Hongo, Tokyo 113-0033, Japan*
[k] *RIKEN, Hirosawa, Wako-shi, Saitama 351-0198, Japan*
[l] *Physics Department, University of Notre Dame, Notre Dame, IN 46556, USA*

Received 14 March 2007; received in revised form 7 April 2007; accepted 10 May 2007

Available online 13 May 2007

Editor: V. Metag

Abstract

The level structures of ^{55}V and ^{55}Ti, the two nuclei with a single nucleon outside the semi-magic $^{54}_{22}\mathrm{Ti}_{32}$ core, have been investigated in order to provide new tests of full pf-shell calculations with the GXPF1A interaction. The addition of a proton does not appear to affect the $N = 32$ shell gap significantly, although comparisons between calculations and experiment at high spins ($I^{\pi} \geqslant 21/2^{-}$) indicate the need for a larger model space for an accurate description of the data in this regime. The energy separation between the $\nu p_{1/2}$ and $\nu f_{5/2}$ orbitals in neutron-rich Ti isotopes is not large enough to result in an $N = 34$ shell gap. However, comparisons between the ^{55}Ti data and the calculations argue for the presence of a sizable $N = 34$ gap in ^{54}Ca.

PACS: 21.60.Cs; 23.20.Lv; 23.90.+w; 27.40.+z

The neutron-rich Ca, Ti, and Cr isotopes have been the focus of many studies during recent years. This effort was prompted primarily by the observation of an $N = 32$ subshell closure in ^{52}Ca [1,2], ^{54}Ti [3], and ^{56}Cr [4], which has been inferred from mounting experimental evidence such as systematic variations in $E(2_1^+)$ energies and $B(E2)$ values in the even–even Ca, Ti and Cr isotopes [2,5–8]. The experimental information is particularly well developed for the Ti and Cr isotopic chains. The two physical quantities are found to be anti-correlated; while the $E(2_1^+)$ energies increase significantly at $N = 32$, the $B(E2)$ strengths are lowest. The situation mirrors that seen for the well-known neutron shell gap at $N = 28$ in nuclei of this region. This new aspect of shell structure in neutron-rich nuclei

* Corresponding author.
E-mail address: janssens@anl.gov (R.V.F. Janssens).
[1] Present address: School of Engineering and Science, University of Paisley, Paisley PA1 2BE, United Kingdom.

0370-2693/$ – see front matter
doi:10.1016/j.physletb.2007.05.014

is understood as resulting from a significant shift in energy of the $\nu f_{5/2}$ orbital caused by a strong proton–neutron monopole interaction [3,9]. When protons are removed from the $\pi f_{7/2}$ shell, the $\nu f_{5/2}$ orbital shifts up in energy relative to the $\nu p_{3/2}$ and $\nu p_{1/2}$ levels due to the weakening of the attractive monopole interaction. Many calculations within the full pf-shell model space have been carried out with different Hamiltonians and most reproduce the features of the yrast level structures fairly well [3,10]. However, the magnitude of the shift in energy of the $\nu f_{5/2}$ orbital appears to be best reproduced by the GXPF1 Hamiltonian developed by Honma et al. [11]. The latter provides a satisfactory description, not only of the variation in the $E(2_1^+)$ energies in the Cr, Ti, and Ca isotopic chains near $N = 32$, but also accounts for the high-spin states in the $^{50,52-54}$Ti isotopes [3,12]. In this context, the absence of the predicted $N = 34$ shell gap between the $\nu p_{1/2}$ and $\nu f_{5/2}$ orbitals in ^{56}Ti was somewhat of a surprise [5,13,14] and suggested that the interaction did not predict the energy shift of the $\nu f_{5/2}$ orbital with sufficient accuracy. This led to a modified GXPF1 interaction, labeled GXPF1A, with a narrower $\nu p_{1/2}$–$\nu f_{5/2}$ gap in the effective single-particle energies. With five $T = 1$ matrix elements involving mainly the $\nu p_{1/2}$ and $\nu f_{5/2}$ single-particle orbitals modified (see Ref. [15] for details), this interaction has provided a consistent description of the known low-lying structures along the entire chain of neutron-rich Ti isotopes, including ^{56}Ti [5,12,13]. It also describes the known Ca isotopes satisfactorily and can account in part for the Cr level structures, although there is also experimental evidence in the $^{56-60}$Cr [6, 16–19] isotopes for the shape-driving role of the $\nu g_{9/2}$ orbital. The present work attempts to provide additional experimental input on the excitation energy of the $\nu p_{1/2}$ and $\nu f_{5/2}$ orbitals by delineating, for the first time, the excited states of ^{55}Ti, the nucleus with one neutron outside the $N = 32$ semi-magic core. Furthermore, the influence of the proton orbitals is also important in accounting for the $N = 32$ shell gap. With a single proton outside the ^{54}Ti core, ^{55}V provides needed information about the impact of protons on the shell gaps in these neutron-rich nuclei just above ^{48}Ca.

Conventional heavy-ion induced fusion–evaporation reactions are ideal for populating high-spin states in proton-rich nuclei, but with proper beam-target combinations, they are also instrumental in accessing neutron-rich nuclei located fairly close to stability, albeit with small cross sections. The technique was exploited in previous studies of the neutron-rich Cr isotopes [6, 16–19]. Thus, with the combination of a ^{9}Be target and ^{48}Ca projectiles, the high-spin states in ^{55}V and ^{55}Ti were populated via the ^{9}Be(^{48}Ca, pn) and ^{9}Be(^{48}Ca, $2p$) reactions, respectively. Just as in Refs. [6,16], these two weak channels had to be resolved from the more abundant xn products through isotopic identification on an event-by-event basis.

The 172-MeV ^{48}Ca beam, delivered by the Argonne Tandem-Linac Accelerator System (ATLAS), was used to bombard a self-supporting ^{9}Be target of 1 mg/cm^2 thickness. Prompt electromagnetic radiation emitted at the target position was detected with the Gammasphere array [20] consisting of 101 Compton-suppressed Ge detectors. Evaporation residues recoiling from the target were separated from the primary beam and

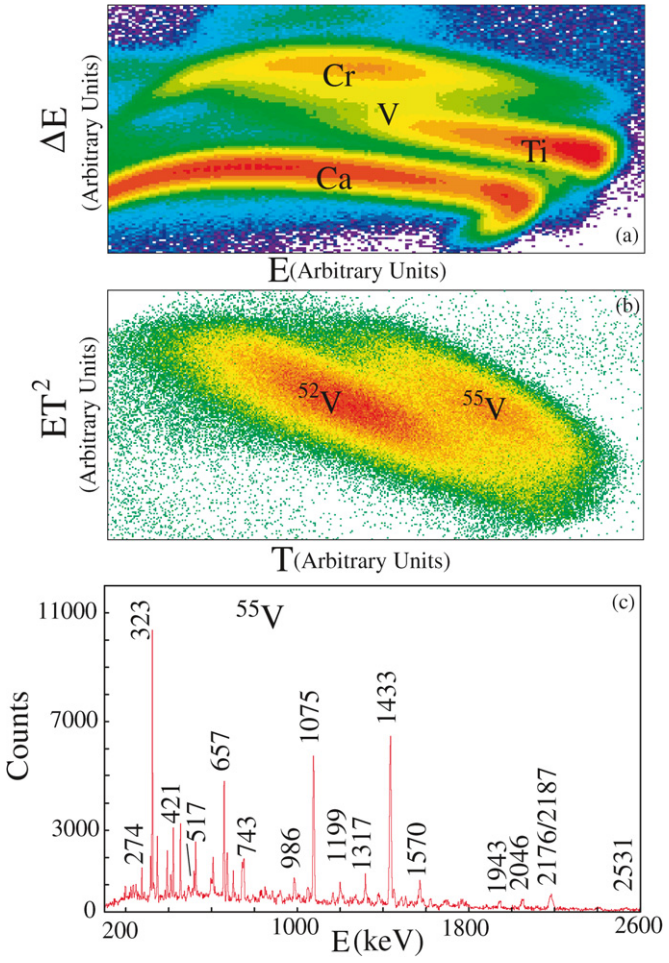

Fig. 1. (a) Two-dimensional plot of E vs. ΔE. The residues with different Z values are well separated. (b) Two-dimensional plot of T vs. ET^2 for element V selected by E vs. ΔE; the residues with mass number 52 and 55 are well separated. (c) Spectrum of γ rays in coincidence with ^{55}V residues selected from plots of E vs. ΔE and T vs. ET^2; the 517-keV peak of ^{55}Cr is the only identified contaminant, which originates from a small leakage of the very strong Cr channels in the V gate.

dispersed in terms of their mass-to-charge ratio (A/Q) by the Fragment Mass Analyzer (FMA) [21]. At the focal plane of the instrument, a parallel-grid avalanche counter (PGAC) measured the horizontal and vertical positions of the recoils and provided timing signals. The residues were subsequently fully stopped in an ionization chamber with three segmented anodes [22], and their energy-loss characteristics were recorded. In order to trigger the data acquisition, one prompt γ ray had to be detected by Gammasphere in coincidence with a residue with $A/Q = 55/18$. A total of 1.4×10^8 events were collected in this way.

Isotopic selection of the residues was achieved by analyzing the energy loss in the three segments of the ionization chamber. This is illustrated in Fig. 1(a) where the energy loss ΔE in the first two segments is plotted against the total energy loss E. The combination of E and the time of flight T of the recoils from the target position to the focal plane, in the form of the ET^2 product, is proportional to the mass of the recoiling ions. The two-dimensional histogram of T versus ET^2, with

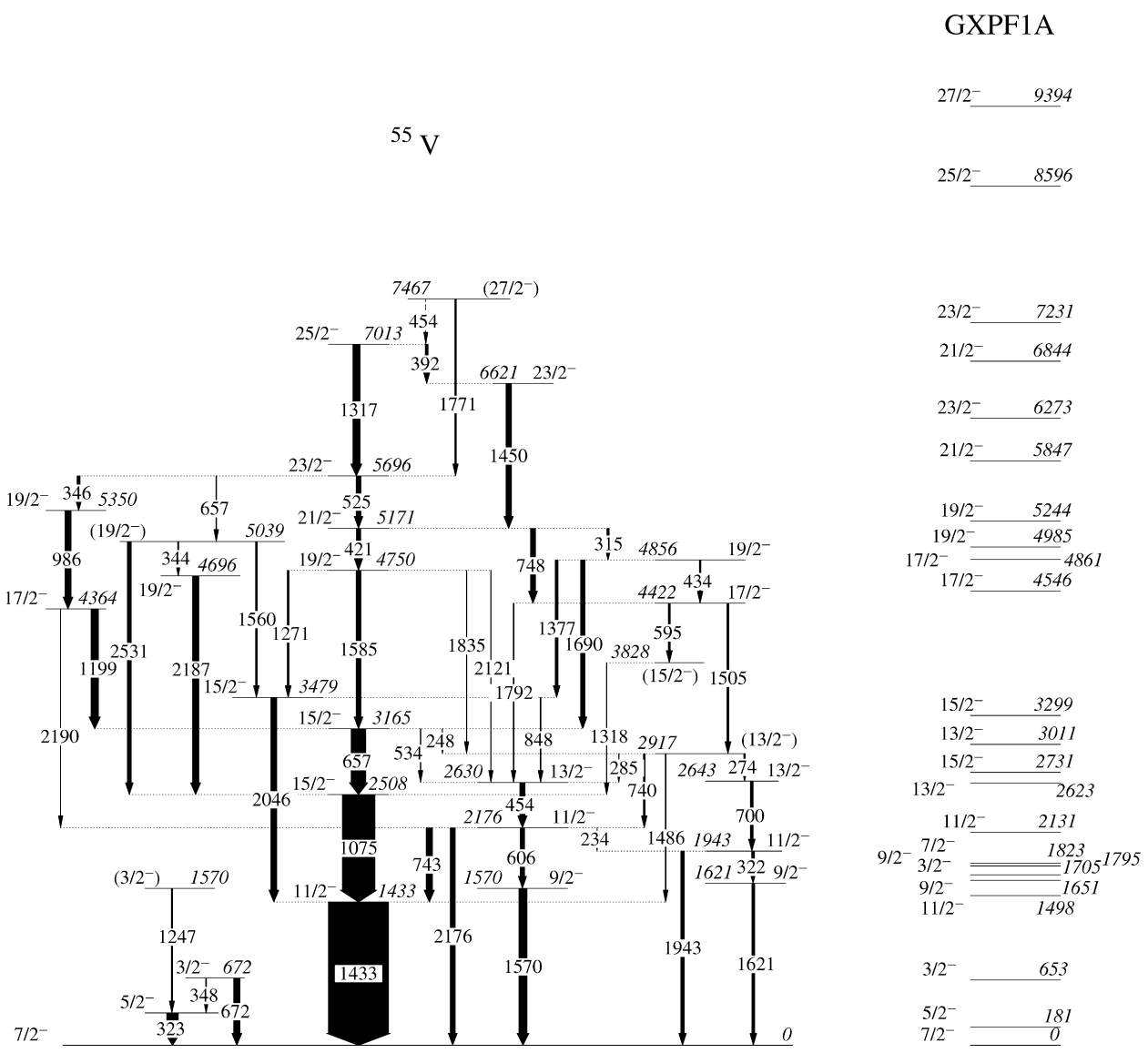

Fig. 2. Proposed level scheme for ^{55}V from the present work. Because of the use of a thin target and the resulting γ decay in-flight, the energies of the strongest transitions are accurate to within 1 keV, while the weaker lines have an associated uncertainty of 2 keV. The widths of the arrows indicate the relative intensities of the transitions. GXPF1A shell-model calculations are given to the right.

an A/Q ratio required to be within the range of 3.02 to 3.09, was used to help resolve charge-state ambiguities. As shown in Fig. 1(b), the mass resolution in such a measurement is sufficient to separate ^{55}V with a ratio $A/Q = 55/18$ from ^{52}V with $A/Q = 52/17$, once a coincidence condition is placed on the V group in Fig. 1(a).

The γ rays in coincidence with the ^{55}V residues can be found in Fig. 1(c), and essentially all the peaks in the spectrum can be assigned to ^{55}V. With the appropriate conditions to select ^{55}V, a $\gamma\gamma$ coincidence matrix was subsequently constructed and analyzed with the Radware software package [23,24] in order to obtain background-subtracted, gated spectra. The level scheme of ^{55}V proposed in Fig. 2 was constructed based on the observed coincidence relationships and on intensity arguments. For transitions with sufficient statistics, multipolarity assignments were made on the basis of the measured angular distribution [6,25] while for weaker transitions, a directional ratio expressed as the ratio of the intensities at angles near 90° (summation of 79°, 81°, 90°, 99° and 101°) and near 150° (summation of 143°, 148° and 163°) was employed. A full account of the results will be presented in a forthcoming publication [26].

As can be seen in Fig. 2, the ^{55}V level scheme is rather complex with many parallel decay pathways. This feature provides the opportunity for many consistency checks. Thus, the ^{55}V level structure is established in the present work with confidence. Some of its specific features are discussed in detail below. The groundstate spin and parity have been adopted as $7/2^-$ based on the β-decay measurement and the systematics presented in Ref. [27]. There are two states with essentially the same energy of 1570 keV. One of these is part of the main level sequence and decays through a 1570-keV γ ray, which is strongly in coincidence with the 606- and 454-keV lines. Another decays through a 1247-keV γ ray to the 323-keV state

observed in β decay [27]. This 1247-keV transition is in coincidence only with the 323-keV γ ray, thereby establishing this 1570-keV level as a distinct state. The remainder of this branch includes the 348-, 323- and 672-keV lines and agrees with the β-decay study of Ref. [27]. The bottom of the main cascade (Fig. 2) is characterized by two strong transitions of 1433 and 1075 keV. Their $E2$ character, established from the measured angular-distribution coefficients, forms the basis for the $11/2^-$ and $15/2^-$ assignments to the 1433- and 2508-keV states. The main feeding of the 2508-keV level occurs through the 657-keV line originating from the 3165-keV state which is also assigned $15/2^-$ quantum numbers. This assignment is based on (a) the measured angular distribution of the 657-keV γ ray, (b) intensity balance considerations, and (c) the presence of other paths feeding in and out of the 3165-keV level that can only be reconciled with one another by postulating a spin and parity of $15/2^-$. For example, the simplest of these pathways involves the 2046- and 1271-keV transitions between the 4750- and 1433-keV levels. Both these transitions can remove at most 2 units of angular momentum, and lifetime considerations combined with the value of the measured directional ratios confirm their $E2$ character. These observations, together with the fact that the measured directional ratio for the 1585-keV link between the 4750- and 3165-keV levels also indicates an $E2$ multipolarity, restrict the quantum numbers of the latter state to $15/2^-$. Similar arguments in favor of this $15/2^-$ assignment also hold for other, more complex pathways. It is worth noting that the level scheme contains four (tentatively five) $19/2^-$ states within less than 700 keV. All of these have been established on the basis of the available coincidence relationships, and quantum numbers have been assigned on the basis of the directional ratios whenever possible, often reinforced by the presence of crossover transitions. Only a small number of transitions could be placed above these $19/2^-$ levels. This is most likely due to the fact that the available yield is rapidly decreasing with spin (because of the choice of reaction) and is fragmented over a large number of pathways.

While the experimental approach outlined above was instrumental in isolating the (p,n) evaporation channel leading to ^{55}V, it was unable to provide information on transitions in ^{55}Ti. Presumably, the cross section for the $(2p)$ channel is smaller in this instance than it was in the successful Cr studies of Refs. [6,16,17]. This may be due to a decrease in the fusion cross section caused by incomplete fusion of the ^{9}Be projectile as observed in other reactions [28,29]. In this case, the level scheme was obtained by combining the results of three measurements. The only knowledge about the ^{55}Ti level structure prior to the present work comes from a β-decay study [14] in which a 593-keV γ ray was reported. In an experiment carried out at Legnaro [30] with a 330-MeV ^{48}Ca beam on a thin ^{238}U target, products from deep inelastic reactions were identified with the PRISMA magnetic spectrometer in coincidence with prompt γ radiation measured with the CLARA array of Compton-suppressed Ge detectors [31]. Two lines with energies 592 and 660 keV were unambiguously associated with transitions in ^{55}Ti nuclei properly identified in Z and A in the spectrometer. Additional, weaker lines at 775 and 1555 keV were tentatively identified

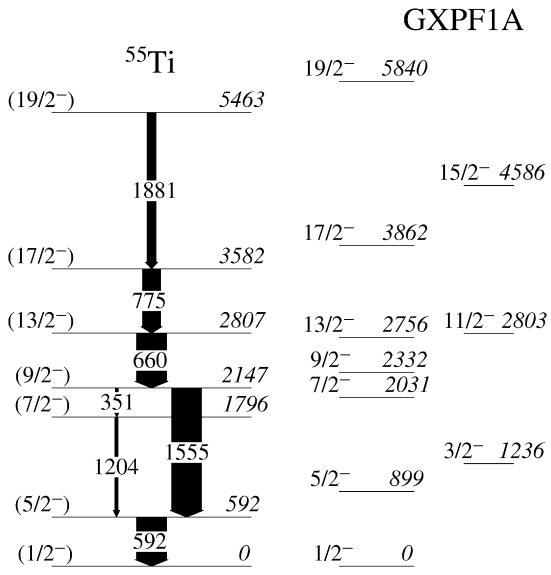

Fig. 3. Proposed level scheme for ^{55}Ti from the present work. The uncertainties on the quoted energies are 0.5 keV. The widths of the arrows indicate the relative intensities of the transitions. GXPF1A shell-model calculations are provided to the right of the level scheme.

as well. Thus, the two data sets are consistent with one another and indicate that the groundstate transition in ^{55}Ti is most likely associated with a 592-keV γ ray. With the information on this and the two other lines discussed above, it was then possible to return to a very large data set obtained with Gammasphere at ATLAS using a thick target and the ^{48}Ca + ^{238}U reaction at 330 MeV. This is the data set used previously to identify first transitions in ^{56}Ti [5], and to confirm and expand the level schemes of ^{53,54}Ti [3,12] and the Cr isotopes [6].

Starting from the transitions mentioned above, the analysis of the $\gamma\gamma\gamma$ coincidence relationships revealed a sequence of mutually coincident lines with energies 592, 1555, 660, 775 and 1881 keV which results in the ^{55}Ti level scheme presented in Fig. 3. A cascade of two γ rays with energies 1204 and 351 keV was identified as well and placed in parallel with the 1555-keV transition. A representative coincidence spectrum of the main cascade is displayed in Fig. 4. The proximity in energy of the 592-keV line to the ^{74}Ge $(n,n'\gamma)$ neutron peak present in all Ge detectors, and the closeness of the 1555-keV γ ray to a 1554-keV transition in ^{50}Ti, one of the strongest reaction products, make it impossible to confirm the order of these two lines on the basis of their measured intensities. Thus, their ordering in Fig. 3 is based solely on the observation of the 592-keV transition in the β-decay measurement, making it the groundstate transition [14]. The presence of the contaminants also resulted in the impossibility of extracting statistically significant angular-correlation information for all the transitions in the cascade. Therefore, all the spin and parity assignments proposed in Fig. 3 are based on the close correspondence between the established levels and calculated states (see below), together with additional considerations such as the information extracted from β decay and the fact that the reaction preferentially feeds yrast states.

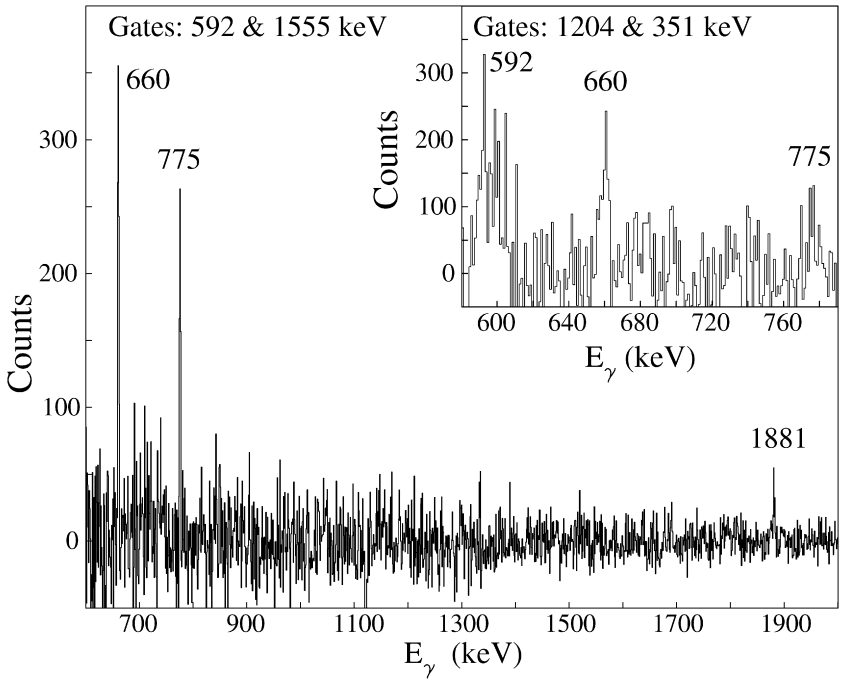

Fig. 4. Sum of double gates on selected γ transitions in ^{55}Ti from data collected with Gammasphere. The shape of the 592-keV γ ray is affected by the $(n, n'\gamma)$ peak; see text for details.

As stated above, the ^{55}V and ^{55}Ti nuclei can be viewed as having respectively a single proton and neutron outside a ^{54}Ti semi-magic core. Thus far, full pf-shell calculations with the GXPF1A effective interaction have provided a satisfactory description of the structural properties associated with the subshell closure at $N = 32$, and they account also for the absence of another subshell closure at $N = 34$ in the Ti and Cr isotopes [5,7]. Comparisons between the detailed experimental level scheme now available for ^{55}V and the GXPF1A calculations can be expected to provide insight in the potential impact on the $N = 32$ shell gap of the occupation of the $\pi f_{7/2}$ orbital by an additional proton. On the other hand, the low-spin yrast structure of ^{55}Ti should involve primarily neutron excitations in the $\nu p_{1/2}$ and $\nu f_{5/2}$ orbitals for which there is considerable debate at this time as the relative location of these single-neutron states determines the presence or absence of an $N = 34$ shell gap in ^{54}Ca, as discussed in Refs. [2,5,7,27].

Full pf-shell calculations have been carried out with the GXPF1A effective interaction for ^{55}V. For clarity, only the lowest two calculated states of each spin and parity are compared with the data on the right-hand side of Fig. 2. In the calculations, the yrast $11/2^-_1$ (1433 keV) and $15/2^-_1$ (2508 keV) states are dominated by the $\pi f^3_{7/2}$ multiplet. Their excitation energies are very close to those of the 2^+_1 (1495 keV) and 4^+_1 (2497 keV) states in ^{54}Ti, which are understood as excitations in the $\pi f^2_{7/2}$ multiplet. Thus, the configuration of this $15/2^-_1$ state can be written properly as $[\pi(f^3_{7/2}) \otimes \nu(f^8_{7/2}p^4_{3/2})]_{15/2^-}$. Any excitation above this level will involve the breaking of the neutron fully-coupled configuration with the promotion of at least one neutron in the $p_{1/2}$ or $f_{5/2}$ state. The calculations indicate that, because of the proximity in energy of these two neutron orbitals, the wavefunctions of most, if not all, states will imply sizeable $p_{1/2}$–$f_{5/2}$ mixing. A satisfactory description of the observed levels is achieved at least up to $I^\pi = 19/2^-$ (see Fig. 2). For example, the wavefunction of the $15/2^-_2$ state is dominated (50%)[2] by the $[\pi(f^3_{7/2}) \otimes \nu(f^8_{7/2}p^3_{3/2}f_{5/2})]_{15/2^-}$ configuration and the 3165-keV energy of this level is reproduced well by the calculated energy of 3299 keV. The calculations also account for the absence of a $15/2^-_2 \rightarrow 11/2^-_1$ transition as it is computed to be three orders of magnitude slower than the $15/2^-_2 \rightarrow 15/2^-_1$ deexcitation which involves only a change in the neutron configuration. Following the sequence of ^{55}V yrast states, it is worth noting that calculations and measurements continue to reflect the presence of the $N = 32$ shell gap. For example, the $19/2^-_1$, 4696-keV level, which is calculated to better than 300 keV, with a wavefunction dominated (42%) by the $[\pi(f^3_{7/2}) \otimes \nu(f^8_{7/2}p^3_{3/2}f_{5/2})]_{19/2^-}$ configuration, deexcites through a $19/2^-_1 \rightarrow 15/2^-_1$ transition of energy (2187 keV) similar to those seen for levels involving a similar predominant $\nu f_{5/2}$ excitation in ^{54}Ti [3]. As will be discussed in detail in Ref. [26], the calculations also predict the presence of additional states with $11/2^-$, $13/2^-$ and $15/2^-$ quantum numbers (not shown for clarity in Fig. 2), with satisfactory agreement with the data: on average these levels are computed within ~500 keV of the data. Above $I^\pi = 19/2^-$, the energy difference between the predictions and the data appears to increase rapidly: the $23/2^-_1$ and $25/2^-_1$ levels are computed too high in energy by 580 and 1580 keV, respectively. This shortcoming is presumably due to the limited model space used in the

[2] In the present discussion, a configuration quoted as dominant implies that all other contributing configurations have probabilities $\leqslant$10%.

calculations, and has similarities with the compression of experimental levels reported in Ref. [6] for ^{58,60}Cr where it was assigned to the impact of the $g_{9/2}$ intruder orbital on the single-particle structure at higher energy.

As discussed in Ref. [27], the spin and parity assignments for the ^{55}Ti groundstate remain uncertain. The $I^\pi = 1/2^-$ values adopted here are based on the results of pf-shell calculations with the GXPF1A interaction which point to a groundstate wavefunction dominated (74%) by the $[\pi(f_{7/2}^2) \otimes \nu(f_{7/2}^8 p_{3/2}^4 p_{1/2})]_{1/2^-}$ configuration. Thus, the ^{55}Ti groundstate can be viewed as the result of the coupling of a $p_{1/2}$ neutron to a ^{54}Ti core. The assignment of $5/2^-$ quantum numbers to the ^{55}Ti first excited state is motivated experimentally by its appreciable direct feeding (∼40%) in the β decay from the $7/2^-$, ^{55}Sc groundstate [14]. The calculations interpret this level in a straightforward manner as resulting from the $^{54}\text{Ti} \otimes \nu f_{5/2}$ coupling, as indicated by the 54% probability of the associated configuration in the wavefunction. The couplings of the $p_{1/2}$ and $f_{5/2}$ neutrons to the 2^+ level of ^{54}Ti are computed to result in non-yrast states, making them difficult to observe in the present measurements. In contrast, the couplings of a $p_{1/2}$ neutron to the ^{54}Ti 4^+ and 6^+ yrast excitations, resulting in the $9/2^-$ and $13/2^-$ states, are computed to be yrast with probabilities of 55% and 72%, respectively, for the configurations $[\pi(f_{7/2}^2) \otimes \nu(f_{7/2}^8 p_{3/2}^4 p_{1/2})]_{9/2^-}$ and $[\pi(f_{7/2}^2) \otimes \nu(f_{7/2}^8 p_{3/2}^4 p_{1/2})]_{13/2^-}$. The $9/2^-$ state exhibits a weak decay branch ($\text{B(M1}; 9/2^- \to 7/2^-)/B(E2; 9/2^- \to 5/2^-) = 1.5(8)\mu_N e^{-2} b^{-2}$) to the $7/2^-$ level. The latter state has a fragmented configuration with the major components being 31% $[\pi(f_{7/2}^2) \otimes \nu(f_{7/2}^8 p_{3/2}^3 p_{1/2} f_{5/2})]_{7/2^-}$ and 28% $[\pi(f_{7/2}^2) \otimes \nu(f_{7/2}^8 p_{3/2}^4 f_{5/2})]_{7/2^-}$. The calculated branching ratio for the decay of the $9/2^-$ level ($\text{B(M1}; 9/2^- \to 7/2^-)/B(E2; 9/2^- \to 5/2^-) = 0.5\mu_N e^{-2} b^{-2}$) compares favorably with the data. The calculations interpret the $17/2^-$ state as the $^{54}\text{Ti}(6^+) \otimes f_{5/2}$ coupling: the probability of the corresponding wavefunction being 56%. In order to generate a $19/2^-$ state, the neutron core has to be broken and a $p_{3/2}$ neutron hole created. This is reflected experimentally in the 1881-keV energy of the $19/2^- \to 17/2^-$ transition, and theoretically in the large probability (74%) of the $[\pi(f_{7/2}^2) \otimes \nu(f_{7/2}^8 p_{3/2}^3 p_{1/2} f_{5/2})]_{19/2^-}$ configuration. While the agreement between experiment and theory for ^{55}Ti level structure can be viewed as satisfactory, it is worth pointing out that the energy difference between the lowest levels with predominant $p_{1/2}$ and $f_{5/2}$ configurations (i.e. the $5/2^- – 1/2^-$ difference) is smaller experimentally than calculated by 307 keV. Thus, it appears that the two single-particle orbitals may be somewhat closer in energy than the GXPF1A Hamiltonian would predict, although other effects may also contribute to this difference (such as the relative positions of the $p_{1/2}$ and $p_{3/2}$ states, for example). The calculations of Fig. 3 correspond to an actual gap of 2.7 MeV between the two single-particle states at $N = 34$. This gap in turn translates in a first excited 2^+ state predicted to lie at 2957 keV in ^{54}Ca. The verification of this excitation energy remains an important experimental challenge.

In summary, excited states in ^{55}V and ^{55}Ti have been populated by utilizing different reaction mechanisms. To first order, the deduced level structures can be understood as resulting from the coupling of a $f_{7/2}$ proton and a $p_{1/2}$ or a $f_{5/2}$ neutron to a ^{54}Ti semi-magic core. Shell-model calculations with the GXPF1A Hamiltonian account for the data reasonably well. Whether a sizeable $N = 34$ shell gap occurs once the last two protons are removed from the $f_{7/2}$ shell remains an intriguing issue demanding experimental input from a study of ^{54}Ca.

Acknowledgements

This work was supported by the US Department of Energy, Office of Nuclear Physics, under Contract No. DE-AC02-06CH11357, by the UK Engineering and Physical Sciences Research Council, by US National Science Foundation Grants Nos. PHY-01-01253, and PHY-0456463, and by Polish Scientific Committee Grant No. 1PO3B 059 29.

References

[1] A. Huck, et al., Phys. Rev. C 31 (1985) 2226.
[2] A. Gade, et al., Phys. Rev. C 74 (2006) 021302(R).
[3] R.V.F. Janssens, et al., Phys. Lett. B 546 (2002) 55.
[4] J.I. Prisciandaro, et al., Phys. Lett. B 510 (2001) 17.
[5] B. Fornal, et al., Phys. Rev. C 70 (2004) 064304.
[6] S. Zhu, et al., Phys. Rev. C 74 (2006) 064315.
[7] D.-C. Dinca, et al., Phys. Rev. C 71 (2005) 041302(R).
[8] A. Bürger, et al., Phys. Lett. B 622 (2005) 29.
[9] T. Otsuka, et al., Phys. Rev. Lett. 87 (2001) 082502.
[10] P.F. Mantica, et al., Phys. Rev. C 67 (2003) 014311.
[11] M. Honma, et al., Phys. Rev. C 65 (2002) 061301(R).
[12] B. Fornal, et al., Phys. Rev. C 72 (2005) 044315.
[13] S.N. Liddick, et al., Phys. Rev. Lett. 92 (2004) 072502.
[14] S.N. Liddick, et al., Phys. Rev. C 70 (2004) 064303.
[15] M. Honma, Eur. Phys. J. A 25 (Suppl. 1) (2005) 499.
[16] S.J. Freeman, et al., Phys. Rev. C 69 (2004) 064301.
[17] A.N. Deacon, et al., Phys. Lett. B 622 (2005) 151.
[18] S.J. Freeman, et al., J. Phys. G 31 (2005) S1465.
[19] A.N. Deacon, PhD Thesis, University of Manchester, 2006.
[20] I.Y. Lee, Nucl. Phys. A 520 (1990) 641c.
[21] C.N. Davids, Nucl. Instrum. Methods Phys. Res. B 70 (1992) 358.
[22] C. Jiang, et al., Nucl. Instrum. Methods Phys. Res. A 554 (2005) 500.
[23] D.C. Radford, Nucl. Instrum. Methods Phys. Res. A 361 (1995) 297.
[24] D.C. Radford, Nucl. Instrum. Methods Phys. Res. A 361 (1995) 306.
[25] V.E. Iacob, G. Duchêne, Nucl. Instrum. Methods Phys. Res. A 399 (1997) 57.
[26] D. Steppenbeck, et al., in preparation.
[27] P.F. Mantica, et al., Phys. Rev. C 68 (2003) 044311.
[28] J.S. Eck, A.R. Omar, J.R. Leigh, T.R. Ophel, Phys. Rev. C 27 (1983) 1807.
[29] M. Dasgupta, et al., Phys. Rev. Lett. 82 (1999) 1395.
[30] B. Fornal, et al., in preparation.
[31] A. Gadea, et al., Eur. Phys. J. A 20 (2004) 193.